NANO EXPRESS　　　　　　　　　　　　　　　　　**Open Access**

A new nanosensor composed of laminated samarium borate and immobilized laccase for phenol determination

Ping Hu, Xinlin Zhou and Qingsheng Wu[*]

Abstract

A new nanosensor composed of laminated samarium borate and immobilized laccase was developed for phenol determination. The laminated samarium borate was synthesized by a mild solid-state-hydrothermal (S-S-H) method without any surfactant or Template. X-ray diffraction (XRD), Fourier transform infrared spectroscopy (FTIR), and scanning electron microscopy (SEM) were used to characterize the samples. The morphology of the as-prepared materials was characterized by SEM, which shows that laminated samarium borate are uniform nanosheets with a layer-by-layer self-assembled single-crystal structure. These laminated samarium borate have typical diameters of 3 ~ 5 μm and the thickness of each layer is in the range of 10 ~ 80 nm. And then, these $SmBO_3$ multilayers were used to immobilize the laccase. The proposed nanosensor composed of laminated samarium borate and immobilized laccase was successfully developed for phenol determination. Cyclic voltammetry were used to study the nanosensor. The proposed nanosensor displayed high sensitivity toward phenolic compounds. The linearity of the nanosensor for the detection of hydroquinone was obtained from 1 to 50 μM with a detection limit of 3×10^{-7} M (based on the S/N = 3).

Keywords: $SmBO_3$; Nanosheets; Laccase; Immobilization; Determination

Background

With the development of the economy, more and more pollutants are eroding the human survival environment. Then the detection and treatment of environmental pollutions have aroused great attentions of scientists. Belonging to multicopper proteins, laccases are widely existed in nature especially fungi [1,2]. It is a phenol oxidase that can catalyze oxidation of many organic pollutants in water [3]. Wan and his group [4] had elaborated the progress on the research of laccases, namely the active center of copper ions, the three-dimensional structure of protein, and its catalytic mechanism. Substrate specificity of laccases was exploited to remove pollutants from the environment without creating the negative effects associated with many other methods [5,6]. It is well known that the enzyme is often easily inactivated in practical applications due to complex environment

conditions, which limit its further industrial application [7,8]. Consequently, immobilized laccases have received much attention from researchers in recent years because of its substantial advantages over free laccases such as continuous reuse, easy separation of the product from the reaction media, easy recovery of the enzyme, and improvement in enzyme stability. Nowadays, many different types of methods have been employed in the immobilization of enzymes, such as adsorption, entrapment, cross-link, and covalent attachment. Recently, it is reported that laccase has been successfully immobilized [9-11] on many different types of supports, such as activated carbon [3], magnetic chitosan [12], alginate chitosan [13], porous glass [14], chitosan/poly(vinyl alcohol) composite nanofibrous membranes [15], cellulose-polyamine composite [16], alginate, kaolinite, polymer beads and membranes polystyrene microspheres, short-range ordered aluminum hydroxide, and so on [17-20]. However, leakage, desorption, and the loss of enzyme activity were major problems in laccase immobilization, which was related to many factors involving the enzyme

* Correspondence: qswu@tongji.edu.cn
Department of Chemistry; Key Laboratory of Yangtze River Water Environment, Ministry of Education, Tongji University, 1239 Siping Road, Shanghai 200092, People's Republic of China

itself, polymer matrix, reaction reagents, and process conditions [9]. Therefore, it is of great interest in developing novel technologies on laccase immobilization to improve catalytic activity of laccase and increase its industrial application.

Among those laccase supports, inorganic materials are more attractive because of their regular structure, good mechanical, chemical, and thermal stabilities [21-23]. Nanomaterials have attracted increasing attention for their novel properties and potential applications with small dimensions [24,25]. Inorganic nanomaterials of rare-earth borate compounds show high vacuum ultraviolet (VUV) transparency and exceptional optical damage thresholds. Acentric lanthanide borate crystals are useful in a wide variety of photonic devices for unique optical, nonlinear optical, laser, electronic, and other physical properties [24,25]. In the past decades, the rare-earth borates are widely used in many fields [26-30] and a number of synthetic methods have been employed to fabricate them. However, many routes suffer from the use of high temperature, tedious processes, and environmental pollution. Therefore, it is still an attractive and necessary topic for the development of environmentally friendly, facile, and reproducible methods to fabricate rare-earth borate nanometer materials.

In this paper, we choose a novel laminated $SmBO_3$ multilayer as support for the immobilization of laccase. The $SmBO_3$ multilayer samples were synthesized via the solid-state-hydrothermal (S-S-H) method, which exhibits many advantages, such as no side products, facile operation, and low cost. Then laccase was immobilized in $SmBO_3$ nanosheets for the fabrication of the nanosensor. The performance of the proposed nanosensor composed of the laminated samarium borate and immobilized laccase in the catalytic determination of phenolic compounds has been investigated in detail.

Methods
Reagents and apparatus
All reagents were analytical grade in the synthesis system. H_3BO_3 (>99.0%), Sm_2O_3 (>99.99%), $Na_2HPO_4 \cdot 12H_2O$ (>99.0%), $C_6H_8O_7 \cdot H_2O$ (>99.8%), hydroquinone (>99.99%), and 2, 6-dimethoxyphenol (>99.99%) were purchased from Shanghai Chemical Reagent Co, Ltd. (Shanghai, China) and used without any purification. Laccase was provided by Shanghai Daidi Industrial Development Co, Ltd. (Shanghai, China) and stored at 4°C before using.

The morphology and structure of the samples were inspected by using a field emission scanning electron microscope (FE-SEM, Hitachi S4800, Tokyo, Japan) at an accelerating voltage of 5 KV. The phase purity and crystallinity of the samples were characterized by X-ray powder diffraction (XRD) performed on a D8 FOCUS

diffractometer (Bruker, Madison, WI, USA) with $CuK\alpha$ radiation ($\lambda = 0.154056$ nm), employing a scanning rate of $0.02° \cdot s^{-1}$, in the 2θ ranges from 10° to 70°. Infrared spectra (4,000 to 400 cm^{-1}) are recorded by Nicolet 5DX Fourier transform infrared spectroscopy (FTIR; Thermo Fisher Scientific, Waltham, MA, USA) equipped with a TGS/PE detector and a silicon beam splitter with 1 cm^{-1} resolution.

Electrochemical experiments were carried out with a CHI-660B electrochemical workstation (Shanghai, China). Measurements were performed at least three times on a glassy carbon electrode (GCE). A conventional three-electrode system was employed, comprising a GCE (3-mm diameter) as the working electrode, a platinum wire as the auxiliary electrode, and an Ag/AgCl (saturated KCl) as the reference electrode. Voltammetric responses were recorded in 50 ml of substrate solutions prepared in PBS buffer solution. First, the modified electrode was activated by several successive voltammetric cycles from −0.20 to 0.80 V. Second, cycle voltammograms (CVs) at the rate of 50 $mV \cdot s^{-1}$ were carried out from −0.20 to 0.80 V after subtracting the background. Finally, the GCE was regenerated by 10 successive cyclic voltammetric sweeps in the blank solution. After several measurements, the GCE should be repolished. All the electrochemical measurements were carried out at room temperature.

Preparation of $SmBO_3$ nanocrystals
Precursor-laminated $SmBO_3$ multilayers were synthesized by solid-state-hydrothermal method. In a typical synthesis, 0.6 mmol Sm_2O_3, 0.72 mmol H_3BO_3, 14 ml deionized water are mixed in a 20-ml-capacity Teflon-lined autoclave. The autoclave is sealed and maintained at 200°C constantly for 36 h and then cooled to room temperature naturally. The precipitation is centrifuged and washed with deionized water several times. Finally, as-obtained products are dried under vacuum at 60°C for 4 h. We propose that the formation processes of $SmBO_3$ in the solid-state-hydrothermal system at 200°C can be assigned to two stages: Sm_2O_3 is first transformed into hydroxide, $Sm(OH)_3$, then the hydroxide interacts with H_3BO_3 to form products. The formation reactions of $SmBO_3$ are proposed and shown in Figure 1.
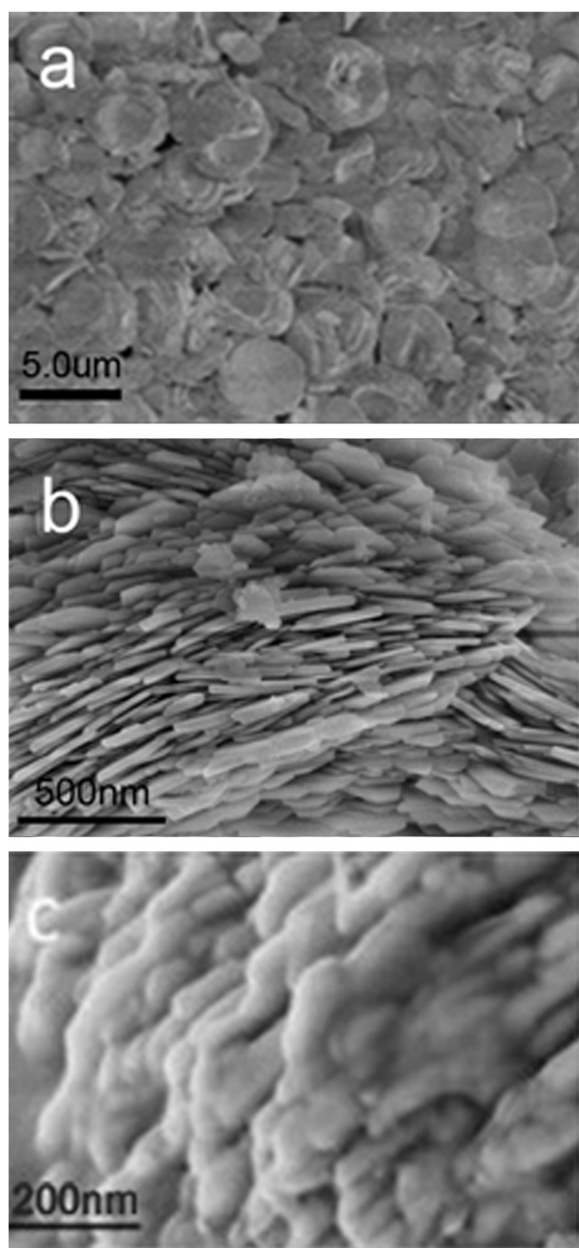
Immobilization of laccase on $SmBO_3$ nanocrystals
The $SmBO_3$ multilayers were employed as carriers for the immobilization of laccase, and the laccase was

$$Sm_2O_3 + H_2O \longrightarrow Sm(OH)_3 \quad (1)$$
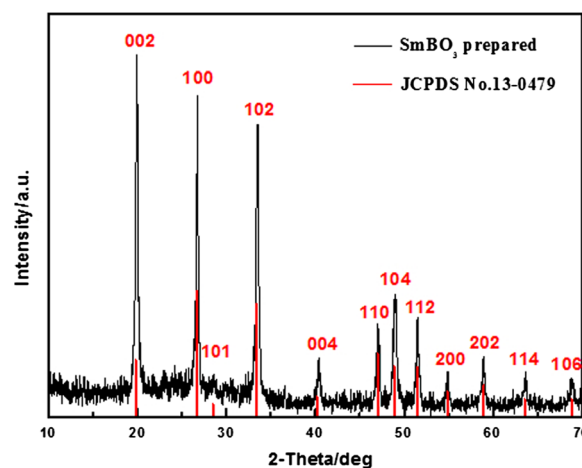
$$Sm(OH)_3 + H_3BO_3 \longrightarrow SmBO_3 \quad (2)$$
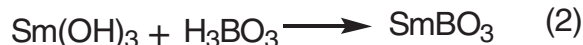
Figure 1 Formation mechanism of $SmBO_3$ in the S-S-H route.

immobilized on these materials by the physical adsorption method. In a typical procedure, 100 mg of $SmBO_3$ support was suspended in 10 ml of phosphate buffer (pH = 7.0) containing a certain amount of laccase (about 20 mg). The mixture of the supports and laccase solution was slowly stirred at room temperature for 12 h. Subsequently, the laccase immobilized on $SmBO_3$ was separated by a centrifuge. Then the samples were washed with 10 ml of buffer solution by shaking for 5 min and separated quickly using a centrifuge. The washing
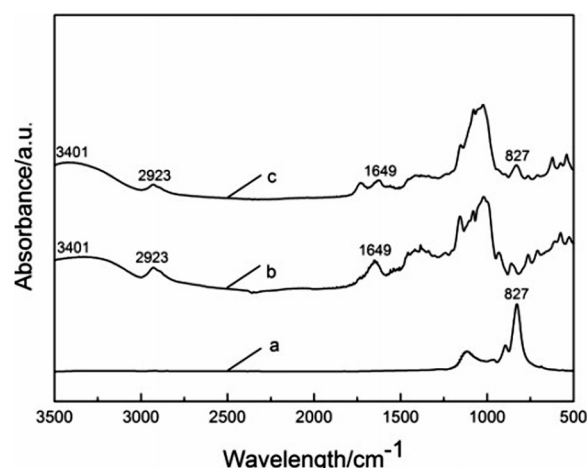

Figure 3 XRD pattern of SmBO₃ via S-S-H method at 200°C for 36 h.

procedure was repeated several times until no protein was detected in the supernatant. Finally, the laccase immobilized by $SmBO_3$ were stored at 4°C before using. The percentage of the immobilized laccase on the $SmBO_3$ samples is in the range of 10.7% ~ 15.2%.

Preparation of the glassy carbon electrode

Ultrasonic agitation was used to disperse 1-mg $SmBO_3$-immobilized laccase into 1-ml Nafion to give a suspension (1 mg $\cdot$ ml^{-1}). Before an experiment, the GCE was polished successively with 0.1-μm γ-Al_2O_3 powder, and then on a polishing cloth. Residual polishing material was removed from the electrode surface by ultrasonic agitation in concentrated HNO_3, distilled water, and absolute ethanol. Then, the GCE was coated with 10 μl of laccase immobilized by $SmBO_3$-Nafion suspension

Figure 2 Typical SEM images of as-prepared SmBO₃ (a), corresponding high-magnified images (b), and immobilized laccase images (c).

Figure 4 FTIR spectra of SmBO₃ (a), laccase (b), and SmBO₃-immobilized lacasse (c).

(1 mg·ml^{-1}) and the solvent evaporated under room temperature for 1 h. The modified electrode was cleaned with distilled water before use.

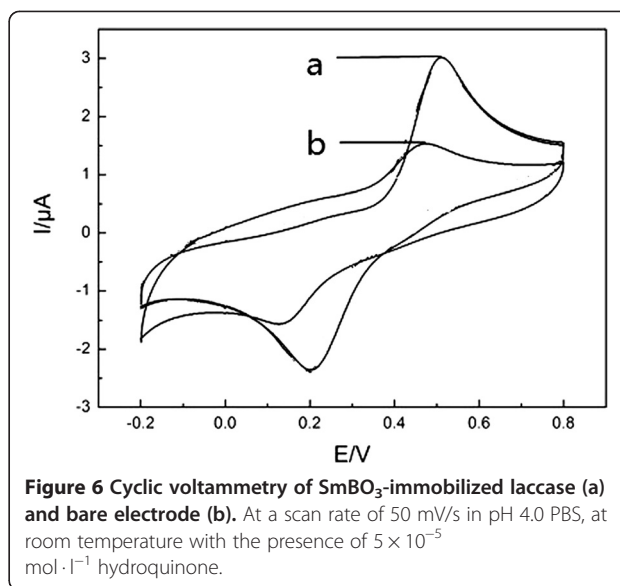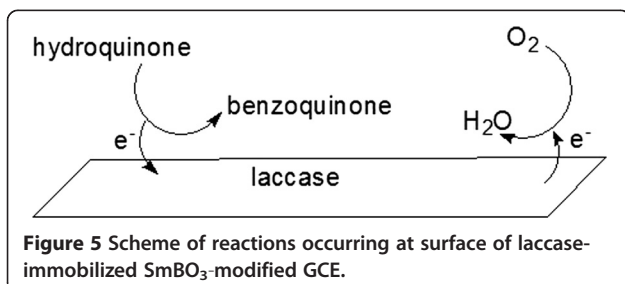## Results and discussion

SEM studies

Figure 2a shows SEM micrographs of as-prepared SmBO$_3$ multilayer obtained via the additive-free S-S-H method at 200°C for 36 h. Figure 2b was the corresponding high-magnified images. The multilayer shapes consist of multi-layer nanosheets. These nanosheets have typical diameters of 3 ~ 5 μm while the thickness of the single layer are in the range of 10 ~ 80 nm. These microparticles are nonaggregated with narrow size distribution. The pseudo-vaterite self-assembled SmBO$_3$ multilayers exhibit advantages in high-ratio surface area and analogy-graphite layer structure, which are favorable for potential application in enzyme immobilization. Figure 2c shows that the laccase was effectively filled among layers of SmBO$_3$ by physical absorption. Inspired by this, we inferred the multilayer structures of SmBO$_3$ suitable for immobilization of other enzymes.

The XRD pattern analysis of as-prepared SmBO$_3$ samples

To ascertain the structure of as-prepared SmBO$_3$ samples, corresponding XRD patterns of samples were investigated and shown in Figure 3. The pattern is inconsistent with aragonite-type, which are indexed in the standard pattern database listed in JCPDS. To make clear the crystal structure, the MDI Jade (5.0 Edition) software was applied to auto index the similar patterns in JCPDS. It was found that the peak positions are in accordance with the primitive-lattice hexagonal phase SmBO$_3$ (No. 13-0479).
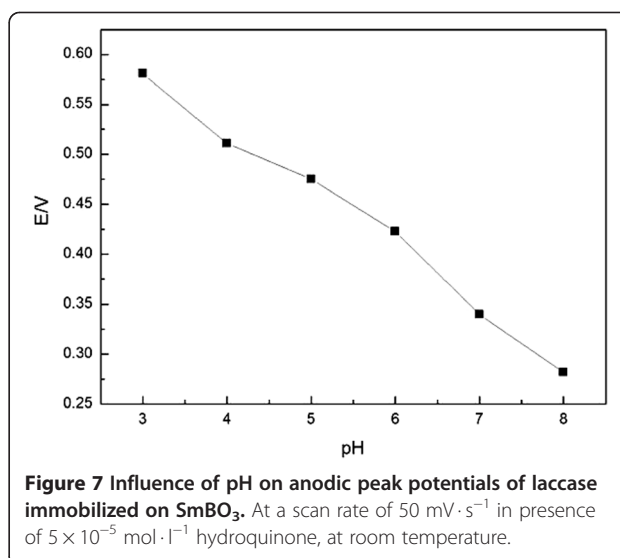
FTIR spectra analysis

Figure 4a shows FTIR spectra of SmBO$_3$ prepared via the S-S-H method at 200°C for 36 h. The absorbance peaks are assigned to the vibration mode of the ring anion B$_3$O$_9$$^{9-}$. A feature of this model is that the B$_3$O$_9$$^{9-}$ group is involving a planar ring with D3 symmetry. The assignment model is proposed in hexagonal LnBO$_3$ as follows: Due to the stretching vibrations of the ring sketch of the cyclic trimeric ion and the terminal B-O and bending vibrations of them, the absorption bands in
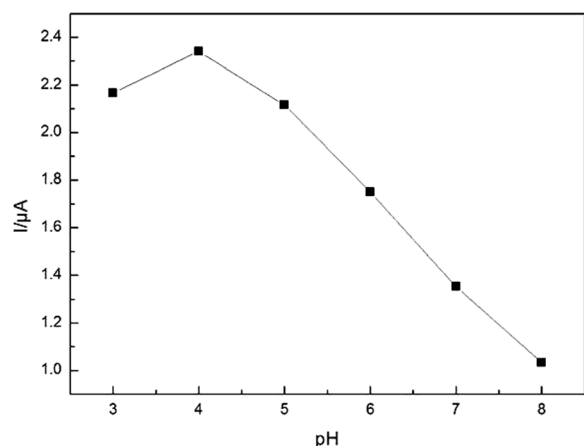
Figure 6 Cyclic voltammetry of SmBO$_3$-immobilized laccase (a) and bare electrode (b). At a scan rate of 50 mV/s in pH 4.0 PBS, at room temperature with the presence of 5×10^{-5} mol·l^{-1} hydroquinone.

the region of 800 to 1,200 cm^{-1} and below 500 cm^{-1}, respectively [31-34]. To investigate the binding between the laccase and the laminated SmBO$_3$ multilayers, FTIR spectra for the laminated SmBO$_3$ multilayers, lacasse, and laminated SmBO$_3$ multilayers with immobilized lac-case were measured.

Figure 4b,c shows the FTIR spectra laccase and SmBO$_3$-immobilized lacasse. Compared to the typical absorption peaks of lacasse at 3,401, 2,923, and 1,649 cm^{-1} and the main absorption peaks of SmBO$_3$ at 1,110, 960, 894, and 827 cm^{-1}, the absorption of SmBO$_3$-immobilized lacasse include all of the above peaks. So it is evident that the lac-case was successfully immobilized on SmBO$_3$ nanosheets. Moreover, it can be seen from Figure 4 that the positions of lacasse and those immobilized in SmBO$_3$ are nearly at
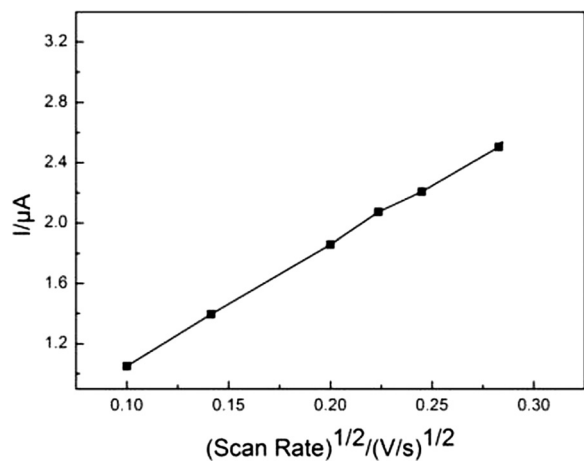
Figure 5 Scheme of reactions occurring at surface of laccase-immobilized SmBO$_3$-modified GCE.

Figure 7 Influence of pH on anodic peak potentials of laccase immobilized on SmBO$_3$. At a scan rate of 50 mV·s^{-1} in presence of 5×10^{-5} mol·l^{-1} hydroquinone, at room temperature.

Figure 8 Influence of pH on anodic peak currents of laccase immobilized on SmBO₃. At a scan rate of 50 mV·s⁻¹ in presence of 5×10^{-5} mol·l⁻¹ hydroquinone, at room temperature.

Figure 10 Calibration graphs of concentration of hydroquinone of laccase-immobilized SmBO₃-modified electrode. a. 5, b. 3, c. 1, d. 0.8, e. 0.5, f. 0.3, g. 0.1, h. 0×10^{-5} mol·l⁻¹.
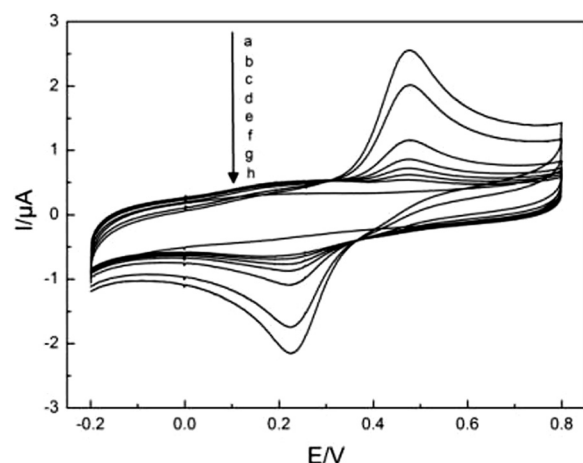
the same place, suggesting that the lacasse retains its native structure in $SmBO_3$-immobilized lacasse.

Electrochemical properties

The response of laccase-immobilized $SmBO_3$ nanosheets for phenolic compound detection is based on the mechanism in which a substrate (hydroquinone in this case), laccase, and oxygen are involved. The enzymatic mechanism involved in laccase-immobilized $SmBO_3$ for phenolic compound detection is the same as the bare laccase [4]. Laccase as one of the multicopper oxidases contains four copper atoms and catalyzes the four-electron reduction of O_2 to H_2O at a trinuclear copper cluster. The catalytic process consists of the oxidation of hydroquinone by
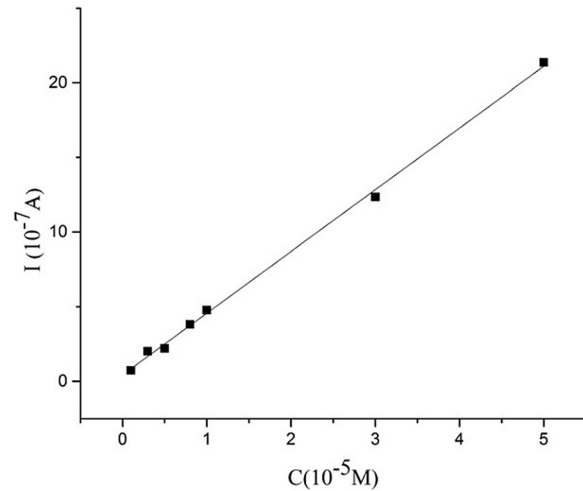
laccase followed with the reduction of O_2 by laccase (Figure 5).

The electrochemical behaviors of laccase-immobilized $SmBO_3$-modified GCE in various solutions were studied using cyclic voltammetry and the results are shown in Figure 6. The laccase-immobilized $SmBO_3$-modified GCE remain its redox behaviors in pH 4.0 PBS at room temperature with the presence of 5×10^{-5} mol·l⁻¹ hydroquinone. The anodic peak currents of laccase-immobilized $SmBO_3$-modified GCE are 3.0 μA. Compared to the anodic peak current of bare electrode which is 1.48 μA, the anodic peak current of modified GCE is at least two times greater. These demonstrate that the electrode of the $SmBO_3$-immobilized laccase has a better sensitivity to the substrate. At the same time, we found that the ΔE of laccase-

Figure 9 Influence of square root of scan rate on anodic peak currents of laccase immobilized on SmBO₃. At a scan rate of 50 mV·s⁻¹ in pH 4.0 PBS, at room temperature in presence of 5×10^{-5} mol·s⁻¹ hydroquinone.

Figure 11 Calibration curve between catalytic current and concentration of hydroquinone in pH 4.0 PBS, at room temperature.

immobilized $SmBO_3$-modified GCE (0.51 V) is larger than bare electrode (0.47 V). According to the Gibbs-Helmholtz equation $\Delta G = -nF\Delta E$, ΔG of the laccase-immobilized $SmBO_3$-modified GCE is smaller than the bare electrode. These results suggest that the reaction occurs on the laccase-immobilized $SmBO_3$ electrode is much easier than the bare electrode.

Optimal parameters

We used $0.2 \ mol \cdot l^{-1}$ $Na_2HPO_4 \cdot 12H_2O$ and $0.1 \ mol \cdot l^{-1}$ $C_6H_8O_7 \cdot H_2O$ solutions to adjust the pH of the buffer solutions from 3.0 to 8.0. Figures 7 and 8 show the relationship between the pH values and the anodic peak potentials, the anodic peak currents from CV, respectively. The potentials shifted negatively with increasing pH value. At the same time, the anodic peak currents increased slightly with increasing pH, and when the pH exceeded 4.0, the anodic peak currents decreased immediately. It may be due to the high oxidation potentials and the serious interference at low pH values. Therefore, pH 4.0 was chosen as the optimum pH in this work.

Cycle voltammograms were employed to investigate the influence of scan rate on hydroquinone oxidation at the laccase-immobilized $SmBO_3$-modified electrode. The results are shown in Figure 9. At scan rates in the range of 0.01 to 0.1 $V \cdot s^{-1}$, the oxidative peak currents of the laccase-immobilized $SmBO_3$-modified electrode in hydroquinone solution increased linearly with the square root of the scan rate, which proved that the electro-oxidation of hydroquinone was a diffusion-controlled process.

Calibration graphs

The anodic peak currents (I_p) of laccase-immobilized $SmBO_3$-modified electrode of the CV are proportional to the concentration of hydroquinone from 1×10^{-6} to $5 \times 10^{-5} \ mol \cdot l^{-1}$. The picture is shown in Figure 10.

The calibration curve under optimal conditions is shown in Figure 11. The linear response range of laccase-immobilized $SmBO_3$-modified electrode to hydroquinone concentration is from 1 to 50 μM with a correlation coefficient of 0.998 ($I = 4.13c +0.42$, $r = 0.998$). The detection limits of the compounds are estimated to be $3 \times 10^{-7} \ mol \cdot l^{-1}$.

Conclusions

In summary, we have demonstrated a nanosensor composed of laminated samarium borate and immobilized laccase for phenol determination. These $SmBO_3$ nanosheets have been successfully prepared via a mild solid-state-hydrothermal method without any surfactant or template, and laccase was successfully immobilized on these multilayers through physical adsorption method. The uniform multilayer-intersected structure could play an important role in the adsorption of laccase. This novel laccase immobilization method based on $SmBO_3$

improved the performance of the laccase for phenol determination. The linear range and bioactivity of laccase-modified electrode can also satisfy the practical application. The present study has enlarged the family of support for laccase immobilization and may provide an efficient approach for phenol determination.

Authors' contributions

PH and XZ carried out the experiments and analyzed the data. PH drafted and revised the paper; QW designed and supervised the whole work. All authors read and approved the final manuscript.

References

1. Baldrian P: **Fungal laccases—occurrence and properties.** *FEMS Microbiol Rev* 2006, **30**:215–242.
2. Durán N, Rosa MA, D'Annibale A, Gianfreda L: **Applications of laccases and tyrosinases (phenoloxidases) immobilized on different supports: a review.** *Enzyme Microb Technol* 2002, **31**:907–931.
3. Lu L, Zhao M, Wang Y: **Immobilization of laccase by alginate-chitosan microcapsules and its use in dye decolorization.** *World J Microbiol Biotechnol* 2007, **23**:159–166.
4. Wan Y-Y, Du Y-M: **Structure and catalytic mechanism of laccases.** *Chemistry* 2007, **70**:662–670.
5. Zhu YF, Kaskel S, Shi JL, Wage T, van Pée KH: **Immobilization of Trametes versicolor laccase on magnetically separable mesoporous silica spheres.** *Chem Mater* 2007, **19**:6408–6413.
6. Savolainen A, Zhang YF, Rochefort D, Holopainen U, Erho T, Virtanen J, Smolander M: **Printing of polymer microcapsules for enzyme immobilization on paper substrate.** *Biomacromolecules* 2011, **12**:2008–2015.
7. Forde J, Tully E, Vakurov A, Gibson TD, Millner P, Fágáin CÓ: **Chemical modification and immobilisation of laccase from trametes hirsuta and from myceliophthora thermophila.** *Enzyme Microb Technol* 2010, **46**:430–437.
8. D'Annibale A, Stazi SR, Vinciguerra V, Mattia ED, Sermanni GG: **Characterization of immobilized laccase from Lentinula edodes and its use in olive-mill wastewater treatment.** *Process Biochem* 1999, **34**:697–706.
9. Wang F, Guo C, Liu HZ, Liu CZ: **Immobilization of Pycnoporus sanguineus laccase by metal affinity adsorption on magnetic chelator particles.** *Chem Technol Biotechnol* 2008, **83**:97–104.
10. Xu XH, Lu P, Zhou YM, Zhao ZZ, Guo MQ: **Laccase immobilized on methylene blue modified mesoporous silica MCM-41/PVA.** *Mater Sci Eng C* 2009, **29**:2160–2164.
11. Areskogh D, Henriksson G: **Immobilisation of laccase for polymerisation of commercial lignosulphonates.** *Process Biochem* 2011, **46**:1071–1075.
12. Davis S, Burns RG: **Covalent immobilization of laccase on activated carbon for phenolic effluent treatment.** *Appl Microbiol Biotechnol* 1992, **37**:474–479.
13. Jiang DS, Long SY, Huang J, Xiao HY, Zhou JY: **Immobilization of Pycnoporus sanguineus laccase on magnetic chitosan microspheres.** *Biochem Eng J* 2005, **25**:15–23.
14. Rogalski J, Dawidowicz A, J'ozwik E: **Immobilization of laccase from Cerrena unicolor on controlled porosity glass.** *J Mol Catal B Enzym* 1999, **6**:29–39.
15. Xu R, Zhou QJ, Li FT, Zhang BR: **Laccase immobilization on chitosan/poly (vinyl alcohol) composite nanofibrous membranes for 2,4-dichlorophenol removal.** *Chem Eng J* 2013, **222**:321–329.

16. Moccelini SK, Franzoi AC, Vieira IC, Dupont J, Scheeren CW: **A novel support for laccase immobilization: cellulose acetate modified with ionic liquid and application in biosensor for methyldopa detection.** *Biosens Bioelectron* 2011, **26**:3549–3554.
17. D'Annibale A, Stazi SR, Vinciguerra V, Sermanni GG: **Oxirane-immobilized Lentinula edodes laccase: stability and phenolics removal efficiency in olive mill waste water.** *J Biotech* 2000, **77**:265–273.
18. Jolivalt C, Brenon S, Caminade E, Mougin C, Pontié M: **Immobilization of laccase from Trametes versicolor on a modified PVDF microfiltration membrane:characterization of the grafted support and application in removing a phenylurea pesticide in wastewater.** *J Membr Sci* 2000, **180**:103–113.
19. Cabaj J, Sołoducho J, Chyla A, Jędrychowska A: **Hybrid phenol biosensor based on modified phenoloxidase electrode.** *Sens Actuators B* 2011, **157**:225–231.
20. Pang HL, Liu J, Hu D, Zhang XH, Chen JH: **Immobilization of laccase onto 1-aminopyrene functionalized carbon nanotubes and their electrocatalytic activity for oxygen reduction.** *Electrochim Acta* 2010, **55**:6611–6616.
21. Zhu YH, Cao HM, Tang LH, Yang XL, Li CZ: **Immobilization of horseradish peroxidase in three-dimensional macroporous TiO_2 matrices for biosensor applications.** *Electrochim Acta* 2009, **54**:2823–2827.
22. Xia YN, Yang PD, Sun Y, Wu Y, Mayers B, Gates B, Yin Y, Kim F, Yan H: **One-dimensional nanostructures: synthesis, characterization, and applications.** *Adv Mater* 2003, **15**:353–389.
23. Cui Y, Liber CM: **Functional nanoscale electronic devices assembled using silicon nanowire building blocks.** *Science* 2001, **291**:851–853.
24. Kolis JW, Giesber HG: **Acentric orthorhombic lanthanide borate crystals, method for making, and applications thereof.** In *U S Patent 2005022,720*. 2005.
25. Giesber HG, Ballato J, Pennington WT, Kolis JW: **Synthesis and characterization of optically nonlinear and light emitting lanthanide borates.** *Inform Sci* 2003, **149**:61–68.
26. Tukia M, Hölsä J, Lastusaari M, Niittykoski J: **Eu^{3+} doped rare earth orthoborates, RBO_3 (R = Y, La and Gd), obtained by combustion synthesis.** *Opt Mater* 2005, **27**:1516–1522.
27. Yang L, Zhou LQ, Huang Y, Tang ZW: **Hydrothermal synthesis of GdBO3: Eu^{3+} nanofibres.** *Mater Lett* 2010, **64**:2704–2706.
28. Yang Z, Wen YL, Sun N, Wang YF, Huang Y, Gao ZH, Tao Y: **Morphologies of $GdBO_3$:Eu^{3+} one-dimensional nanomaterials.** *J Alloys Compd* 2010, **489**:L9–L12.
29. Kim T, Kang S: **Hydrothermal synthesis and photoluminescence properties of nano-crystalline $GdBO_3$:Eu^{3+} phosphor.** *Mater Res Bull* 2005, **40**:1945–1954.
30. Jiang XC, Sun LD, Yan CH: **Ordered nanosheet-based YBO_3:Eu^{3+} assemblies: synthesis and tunable luminescent properties.** *J Phys Chem B* 2004, **108**(11):3387–3390.
31. Ma J, Wu QS, Ding YP, Chen Y: **Assembled synthesis and phase transition of pseudovaterite $NdBO_3$ layer-by-layer single-crystal nanopancakes via an oxides-hydrothermal route.** *Cryst Growth Des* 2007, **7**:1553–1560.
32. Ma J, Wu QS, Chen Y, Chen YJ: **A synthesis strategy for various pseudovaterite $LnBO_3$ nanosheets via oxides-hydrothermal route.** *Solid State Sci* 2010, **12**(4):503–508.
33. Ren M, Lin JH, Dong Y, Yang LQ, Su MZ: **Structure and phase transition of $GdBO_3$.** *Chem Mater* 1999, **11**(6):1576–1580.
34. Lin JH, Sheptyakov D, Wang YX, Allenspach P: **Orthoborates: a neutron diffraction study.** *Chem Mater* 2004, **16**:2418–2424.